AGU PUBLICATIONS

JGR

Journal of Geophysical Research: Solid Earth

RESEARCH ARTICLE

10.1002/2017JB014546

Key Points:

- Mantle lithosphere rheology can control the burial and exhumation of crustal rocks
- Viscous removal of a weaker continental mantle lithosphere may yield high-pressure/low-temperature exhumation
- Ultrahigh-pressure/high-temperature metamorphic rocks may be prevalent in subduction of a stronger continental mantle lithosphere

Supporting Information:

- Supporting Information S1

Correspondence to:
O. H. Göğüş,
goguso@itu.edu.tr

Citation:
Bodur, Ö. F., Göğüş, O. H., Pysklywec, R. N., & Okay, A. I. (2018). Mantle lithosphere rheology, vertical tectonics, and the exhumation of (U)HP rocks. *Journal of Geophysical Research: Solid Earth*, *123*, 1824–1839. https://doi.org/10.1002/2017JB014546

Received 19 FEB 2017
Accepted 15 JAN 2018
Accepted article online 20 JAN 2018
Published online 7 FEB 2018

Mantle Lithosphere Rheology, Vertical Tectonics, and the Exhumation of (U)HP Rocks

Ömer F. Bodur[1,2,3], Oğuz H. Göğüş[1], Russell N. Pysklywec[4], and Aral I. Okay[1]

[1]Eurasia Institute of Earth Sciences, Istanbul Technical University, Istanbul, Turkey, [2]Department of Geophysics, Kandilli Observatory and Earthquake Research Institute, Boğaziçi University, Istanbul, Turkey, [3]Now at EarthByte Group and Basin GENESIS Hub, School of Geosciences, University of Sydney, New South Wales, Australia, [4]Department of Earth Sciences, University of Toronto, Toronto, Ontario, Canada

Abstract Numerical modeling results indicate that mantle lithosphere rheology can influence the pressure-temperature-time (P-T-t) trajectories of continental crust subducted and exhumed during the onset of continental collision. Exhumation of ultrahigh-pressure (~35 kbar)/high-temperature (~750°C) metamorphic rocks is more prevalent in models with stronger continental mantle lithosphere (e.g., dry), whereas high-pressure (~9–22 kbar)/low-temperature (350°C–630°C) metamorphic rocks occur in models with weaker rheology (e.g., hydrated) for the same layer. In the latter case, the buried crustal rocks can remain encased in ablatively subducting mantle lithosphere, reach only moderate temperatures, and exhume by dripping/detachment of the lithospheric root. In this transition from subduction to a dripping style of "vertical tectonics," burial and exhumation of crustal rocks are driven without imposed far-field plate convergence. The model results are compared against thermobarometric P-T estimates from major (ultra) high-pressure metamorphic terranes. We propose that the exhumation of high-pressure/low-temperature metamorphic rocks in Tavşanlı and Afyon zones in western Anatolia may be caused by viscous dripping of mantle lithosphere suggesting a weaker continental mantle lithosphere, whereas (ultra)high-pressure exhumation (e.g., Dabie Shan-eastern China and Dora Maira-western Alps) may be associated with plate-like subduction. In the latter case, the slab is much stronger and deformation is localized to the subduction interface along which rocks are buried to >100 km depth before they are exhumed to the near surface.

1. Introduction

Since the discovery of coesite in Western Alps (Chopin, 1984), ultrahigh-pressure rocks have been considered as the evidence of plate subduction. It is the key process driving both the geochemical and thermal mixing of the planet Earth and is responsible for many ultrahigh-pressure occurrences found around the globe (Liou et al., 2004). Blueschist and eclogite facies rocks are found chiefly in Phanerozoic orogenic belts such as the Alpine orogen. For instance, exposed crustal rocks in Tavşanlı zone of western Anatolia experienced high-pressure/low-temperature (HP/LT) metamorphism (up to 24 ± 3 kbar, 430 ± 30°C) at ~80 Ma suggesting a burial down to ~80 km depth following northward subduction of the intervening Tethyan ocean (Okay, 2002; Plunder et al., 2015; Sherlock et al., 1999). Along the same subduction system, Afyon zone metamorphic rocks experienced pressure and temperature conditions of 6–9 kbar and 350°C (Candan et al., 2005) between 70 and 65 Ma (Pourteau et al., 2013), implying a burial to 21–32 km depth before they exhume to the surface. Other examples of (ultra)high-pressure metamorphism -will be denoted as U(HP) hereinafter- are found in the Dora Maira (Rubatto & Hermann, 2001) and Shistes Lustrés (Agard et al., 2001) of western Alps, Western Gneiss complex of the Norwegian Caledonides (Andersen et al., 1991), Dabie Shan in eastern China (Liu et al., 2004; Okay, Şengör, & Satır, 1993), Kaghan (Parrish et al., 2006), and Tso Morari (Mukherjee et al., 2003) in western Himalaya, Kokchetav Massif (Sobolev & Shatsky, 1990) in northern Kazakhstan, and Erzgebirge (Massonne, 2003) in northwest of Bohemian Massif.

Various geodynamic mechanisms have been put forward to account for burial and exhumation of crustal rocks (Burov et al., 2014; Hacker & Gerya, 2013; Liou et al., 2004; Warren, 2013). For the tectonic setting transitioning from oceanic plate subduction to continental collision, buried crustal rocks may exhume as a coherent block by detachment of a subducted slab (Duretz et al., 2012). In a subduction channel-flow mechanism, crustal rocks are buried and circulated within a subduction-driven channel before they exhume to the near surface (Burov et al., 2001; Li & Gerya, 2009; Warren, Beaumont, & Jamieson, 2008a, 2008b; Yamato et al., 2007, 2008). Delamination of mantle lithosphere from overlying crust may also yield transient slab migration and sublithospheric mantle upwelling that can promote exhumation of buried rocks (Duretz & Gerya, 2013; Göğüş et al., 2011, 2016; Göğüş & Pysklywec, 2008a, 2008b). A similar slab retreat process may drive exhumation of buoyant continental crustal blocks from the deep mantle (Brun & Faccenna, 2008; Tirel et al., 2013).

These mechanisms are all related to plate-like behavior of the continental plate subduction. Essentially, the subduction is coherent and there is no disturbance on the upper plate. Alternate styles of lithospheric deformation for the mature stage of orogenesis have been proposed (Pysklywec et al., 2002, 2010). These assume that lower parts of the subducting lithosphere may show a transition from plate-like consumption to a viscous "dripping" type behavior of the subducted lithospheric root. This change in behavior may be activated by continental thickening and is not related to chemical heterogeneities. The process is mainly driven by rheological changes that arise within the lithosphere during progressive subduction. This is consistent with the geodynamic scenario that have been put forward on the basis of the burial and exhumation of UHP metamorphic rocks in Norwegian Caledonides (Andersen et al., 1991) and Dabie Shan (Okay & Şengör, 1992).

Inferences from geodynamic modeling studies suggest that mantle lithosphere rheology plays an important role in controlling orogenic processes (Burov & Yamato, 2008; Gray & Pysklywec, 2013; Pysklywec et al., 2000). Viscous deformation (i.e., Rayleigh-Taylor instability) has been investigated by numerical (England & Houseman, 1989; Göğüş et al., 2017; Göğüş & Pysklywec, 2008b; Houseman & Molnar, 1997; Molnar et al., 1998) and analogue experiments (Pysklywec et al., 2010; Pysklywec & Cruden, 2004). These studies inherently suggest geometrically symmetric evolution of the surface and crustal deformation patterns. Alternatively, plastic deformation has been suggested to explain the distinct asymmetry in most collisional orogens (Beaumont et al., 1996; Willett et al., 1993). Preexisting asymmetric geometry can also produce asymmetric features in collision.

In this work, we investigate the process of burial and exhumation of crustal rocks in an orogenic system (e.g., Alpine-Himalayan orogenic belt). We test different rheologies (weak versus strong) for continental mantle lithosphere of both upper and lower plate in order to understand the role of mantle lithosphere rheology on the subduction style and the burial-exhumation process. We also vary the imposed plate convergence velocities for each rheological model to further investigate problem.

2. Model Configuration

2.1. Governing Equations

Numerical geodynamic experiments use an arbitrary Lagrangian-Eulerian finite element code with viscoplastic deformation written by (Fullsack, 1995). Assuming an incompressible flow in 2-D, the governing equations for thermo-mechanical computation include conservation of mass, momentum, and internal energy, which are described below:

$$\nabla . v = 0, \tag{1}$$

$$\nabla\left(\sigma_{ij}\right) + \rho g = 0, \tag{2}$$

$$\rho c_p \left(\frac{\partial T}{\partial t} + v \cdot \nabla T\right) = k \nabla^2 T + \rho H, \tag{3}$$

The equation of state is activated by the equation below:

$$\rho = \rho_0 [1 - \alpha (T - T_0)], \tag{4}$$

In equations (1)–(4), ρ, T, and u represent density, temperature, and velocities, respectively. Likewise, g, α, c_p, k, H, and t are variables symbolizing gravitational acceleration (m^2 s^{-1}), thermal expansivity (K^{-1}), heat capacity at constant pressure (J kg^{-1} K^{-1}), thermal conductivity (W m^{-1} K^{-1}), rate of internal heat production per unit mass (W kg^{-1}), and time, respectively. The stress tensor in equation (2) includes two components as follows:

$$\sigma_{ij} = \sigma_{ij}^{'} - P \delta_{ij}, \tag{5}$$

Table 1
Physical Parameters for EXP 1–4

	Reference model	Continental crust[1]	Continental mantle lithosphere[2]	Oceanic lithosphere[3]	Asthenospheric mantle[2]
A	Viscosity parameter	1.1×10^{-28} $Pa^{-4/s}$	4.168×10^{-4} $Pa^{-1/s}$	-	5.495×10^{-25} $Pa^{-4.48/s}$
n	Power exponent	4.0	1	-	4.48
Q	Activation energy	223 kJ mol^{-1}	498 kJ mol^{-1}	-	498 kJ mol^{-1}
ϕ	Internal angle of friction	15°-2°	15°-2°	15°-2°	15°-2°
ρ_o	Reference density	2,800 kg m^{-3}	3,300 kg m^{-3}	3,310 kg m^{-3}	3,280 kg m^{-3}
T_o	Reference temperature	500 K	750 K	750 K	750 K
c_0	Cohesion	10 MPa	0 MPa	20 MPa	0 MPa
α	Coefficient of thermal expansion	3.0×10^{-5} K^{-1}	2.0×10^{-5} K^{-1}	2.0×10^{-5} K^{-1}	2.0×10^{-5} K^{-1}
C	Heat capacity	750 J kg^{-1} K^{-1}	1,250 J kg^{-1} K^{-1}	1,250 J kg^{-1} K^{-1}	1,250 J kg^{-1} K^{-1}
k	Thermal conductivity	2.25 W m^{-1} K^{-1}	2.25 W m^{-1} K^{-1}	2.25 W m^{-1} K^{-1}	2.25 W m^{-1} K^{-1}

Note. References for viscosity parameters are (1) wet quartzite (Gleason & Tullis, 1995) and (2) Aheim dunite (Chopra & Paterson, 1984) (for Newtonian creep we use n = 1). Cohesion of the oceanic lithosphere is from (3) Choi et al. (2013). Thermal conductivity used in numerical models (2.25 W m^{-1} K^{-1}) is an average value derived from laser-flash analysis (Whittington et al., 2009). Other thermal parameters are assumed to be constant. But their sensitivity on the results may be tested in future experiments.

where σ'_{ij} represents deviatoric stress tensor and P stands for applied pressure (in case of an incompressible fluid, $P = -\frac{1}{3}\sigma_{ii}$). It is also important to note that viscoplastic deformation of the materials is executed at the lesser value of either the yield stress σ_{yield} or viscous stress σ_{viscous} for each computation at the grid. This enables the materials to deform at a stress level as low as possible. This can be shown as below:

$$\sigma'_{ij} = \min\left(\sigma_{\text{yield}}; \sigma_{\text{viscous}}\right), \tag{6}$$

Drucker-Prager yield law is used for depth-dependent (provided by the pressure term) frictional plastic yield stress, which is similar to the Coulomb criterion in plane strain (Fullsack, 1995):

$$\sigma_{\text{yield}} = P\sin\phi + c_o, \tag{7}$$

In equation (7) Φ and c_o stand for internal angle of friction and cohesion, respectively. For the crust and mantle, an empirical strain softening for plastic deformation is achieved by decreasing the effective internal angle of friction from ϕ = 15° to ϕ= 2° over the range $0.5 < \varepsilon < 1.5$ where ε is the total strain (see Table 1). This method has been widely used in the literature to account for high strained zones prevalent in major U(HP) terranes (Beaumont et al., 2009; Gray & Pysklywec, 2012; Pysklywec et al., 2010; Terry & Robinson, 2004) and implicitly includes the effect of pore fluid pressure (P_f).

The equation for viscous stress is shown below:

$$\sigma_{\text{viscous}} = 2\eta_e\dot{\epsilon} \tag{8}$$

The effective viscosity η_e of the materials for power law rheology is defined as:

$$\eta_e(\dot{\epsilon}, T) = GA^{\frac{-1}{n}}\dot{\epsilon}^{\frac{1-n}{n}}e^{\frac{Q}{nRT}}, \tag{9}$$

where

$$G = \left(3^{\frac{-(n+1)}{2n}}2^{\frac{(1-n)}{n}}\right), \tag{10}$$

The variables $\dot{\epsilon}$, A, Q, n, and R represent strain rate (s^{-1}), viscosity parameter (MPa^{-n} s^{-1}), activation energy from uniaxial laboratory experiments (kJ mol^{-1}), power law exponent, and ideal gas constant, respectively. G is used for the conversion of the uniaxial laboratory data to a condition of stress, which is not dependent on the coordinate system (Pysklywec et al., 2002).

2.2. Model Geometry

The investigated tectonic configuration is an idealized model of a transition from oceanic subduction to continental collision (Figure 1). In the numerical models, 150 km thick continental lithosphere (ρ_o = 3,300 kg m^{-3}

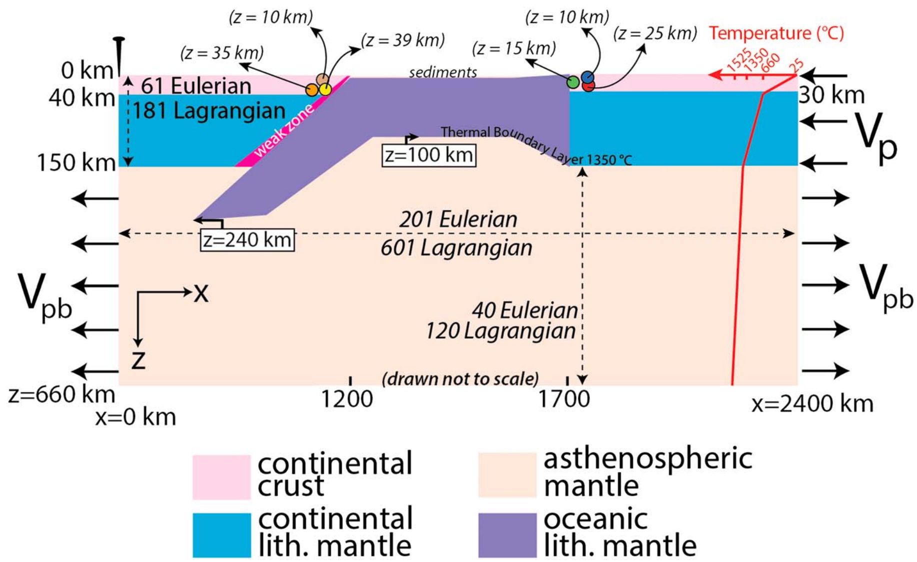

Figure 1. Illustration of the numerical model geometry, the geotherm, distribution of the Lagrangian and Eulerian grids, and initial positions of tracked Lagrangian nodes representative of crustal rocks. The Lagrangian grid tracks the deformation and physical histories of materials (pressure, temperature).

for continental mantle lithosphere) has 40 km thick crust (ρ_o = 2,800 kg m^{-3}) in the upper plate, 30 km thick crust (ρ_o = 2,800 kg m^{-3}) in the lower (subducting) continental plate representing a continental margin geometry that may have a thinner crust. The reference density of continental crust is an approximation to wet quartzite type continental crust (Beaumont et al., 2009). The thickness of the oceanic lithosphere is 100 km (ρ_o = 3,310 kg m^{-3}), and the numerical models start from a stage where subduction of oceanic plate has been progressing and the tip of the oceanic slab has reached to 240 km depth in the asthenospheric mantle (ρ_o = 3,280 kg m^{-3}). The subduction of oceanic plate is promoted by prescribing a weak zone in the subduction interface deforming at constant viscosity, which corresponds to the lower limit of viscosity range of the numerical models (5×10^{19} Pa s – 1×10^{22} Pa s using a reference strain rate of 10^{-15} s^{-1}). The density of the weak zone is the same with continental mantle lithosphere.

Both Lagrangian and Eulerian grids are used for computation. As pressure and velocities are computed from Stokes equation on the Eulerian grid, the accumulated strain and other thermal and mechanical history of the materials (temperature, pressure) are recorded on the Lagrangian grid which is deforming accordingly. Updated positions of the fields from the Lagrangian grid are passed back to the Eulerian grid for the following computations. There are 601 Lagrangian grid lines in the horizontal direction. The model resolution in the lithosphere (down to 150 km depth) is 0.83 km vertically (181 Lagrangian grid lines) and 4 km horizontally (601 Lagrangian grid lines). Below this depth, the resolution changes to 4.25 km vertically but stays the same laterally.

A series of experiments are performed to investigate the P-T-t paths of crustal rocks in a system transitioning from oceanic subduction to continental collision. We track Lagrangian nodes representing parcels of crustal rocks from the subducting plate (red particle at 25 km depth, green particle at 15 km depth, and blue particle at 10 km depth) and overriding plate (orange particle at 35 km depth, brown particle at 10 km depth, and yellow particle at 39 km depth). These Lagrangian nodes are selected from rocks showing the deepest burial and notable exhumation. We calculate lithostatic pressures of tracked nodes.

2.3. Material Rheologies

For rheological calculations, we use laboratory measurements based on a viscous flow law and depth-dependent frictional plastic deformation with strain softening.

In the first set of experiments (EXP 1–4), a viscoplastic mantle lithosphere rheology (using Newtonian creep n = 1 and 0 MPa cohesion) is used for deformation of the continental mantle lithosphere. We use Newtonian

Table 2
Description of Varied Parameters for Each Experiment and Resulting Subduction Style

Experiments	Rheology of continental mantle lithosphere of upper and lower plates, imposed convergence velocity, and resulting subduction style
EXP 1 (Reference Model)	Viscoplastic rheology, $V_x = 0$ cm yr^{-1} *(ablative subduction).*
EXP 2	Viscoplastic rheology, $V_x = 1$ cm yr^{-1} *(ablative subduction).*
EXP 3	Viscoplastic rheology, $V_x = 2$ cm yr^{-1} *(ablative subduction).*
EXP 4	Viscoplastic rheology, $V_x = 3$ cm yr^{-1} *(ablative subduction).*
EXP 5	Frictional plastic rheology with 20 MPa cohesion (c_0) (viscous parameters are deactivated), $V_x = 0$ cm yr^{-1}. *Effectively isoviscous, plate-like subduction. Much of the deformation is localized in subduction interface.*
EXP 6	Frictional plastic rheology with 20 MPa cohesion (c_0) (viscous parameters are deactivated), $V_x = 5$ cm yr^{-1}. *Effectively isoviscous, plate-like subduction. Much of the deformation is localized in subduction interface.*

rheology for viscous deformation for a number of reasons. First, experiments using non-Newtonian rheology ($n > 1$) showed that the dripping of the continental lithospheric mantle does not develop in conjunction with the subduction of the oceanic slab. Second, it was shown that in lower parts of continental mantle lithosphere, diffusion creep mechanism can be the dominant process for the deformation (Liao et al., 2017). This basically assumes that continental lithosphere may be hydrated by various processes (e.g., oceanic plate subduction).

An effective oceanic subduction is achieved by using only frictional plastic rheology with 20 MPa cohesion for the oceanic lithosphere. These settings are approximations for the Neo-Tethyan oceanic subduction which was suggested to be controlled by a strong and cold oceanic slab (Okay et al., 1998).

The initial reference density contrast between continental mantle lithosphere and asthenospheric mantle is 20 kg m^{-3}. This is based on the idea that in tectonically younger regions (especially in Phanerozoic) that have relatively younger lithospheric compositions (e.g., Alpine-Himalayan orogeny), the density of the asthenosphere can be lesser than the overlying mantle lithosphere (O'Reilly et al., 2001).

The rheological parameters of the continental crust, continental mantle lithosphere, oceanic lithosphere, and the asthenospheric mantle for reference model (EXP 1) and models using same rheologies but different convergence velocities (EXP 2–4) are described in Table 1. We also examine frictional plastic rheology for continental lithospheric mantle by intentionally deactivating the viscous parameters in EXP 5–6.

EXP 1–4 may be viewed as hydrated (weak) continental mantle lithosphere and EXP 5–6 as dry (strong) continental mantle lithosphere. However, the strength of the lithosphere may also vary due to other factors (e.g., preexisting heterogeneities). The list of all numerical models with parameters varying from the reference model is given in Table 2.

2.4. Velocity Boundary Conditions

The model has a free top surface, allowing the topography to develop as the model evolves. When there is any imposed plate convergence, the velocity boundary conditions are described as a constant inflow from the top to 150 km depth at the right boundary with constant outflow imposed from beneath the lithosphere down to 660 km depth through both sides. The magnitude of the outflow is determined by the rule that the volume of the material inside the box must be constant. The lithosphere on the left margin is held fixed (pinned) for all models. We also examined the free slip boundary condition on the left wall and got very similar results, suggesting that the models are not forced to give any specific subduction style (e.g., slab rollback). If there is no imposed plate convergence, then there is no in/outflux; therefore, sides are free slip. In all experiments, the bottom boundary is no slip, and no material is allowed to penetrate from beneath.

2.5. Temperature Initial/Boundary Conditions

We use a superadiabatic geotherm tuned to give elevated temperatures at the oceanic region, which assumes a lithosphere-asthenosphere thermal boundary layer. More specifically, the temperature at the surface is 25°C, increases to 660°C at the Moho (at 30 km) on the subducting plate. This gives 22°C km^{-1} geotherm corresponding to 900°C beneath 40 km of crust on the upper plate. The temperature increases to 1,350°C at the base of the mantle lithosphere on both sides and up to 1,525°C at the bottom of the model. The surface and bottom temperatures are held constant throughout the experiments, and the heat flux across the side boundaries is zero. Initial temperature profile is the same in all experiments. The imposed temperature profile may serve as enhancing the strength of buoyancy forces in the system in a way that convection at the margin and asthenosphere may be vigorous during model evolution. Thermal properties of materials (i.e., heat capacity, thermal conductivity, and thermal expansion coefficient) for crust and mantle are shown in Table 1. We give the varied parameters for each experiment in Table 2. We do not impose shear heating and melting in the numerical models.

The reference densities are used as an input when calculating the pressure conditions of buried rocks, because temperature effect on density and lithostatic pressure was relatively minor. No radiogenic heat is produced in the crust or mantle, but the surface heat flow in the numerical experiments (~50 mW m^{-2}) is representative of a typical continental margin (Davies, 2013). The thermal properties of the crust and mantle are assumed to be invariant. We use an average value for conductivity of materials (2.25 W m^{-1} K^{-1}) to represent the distribution of heat during model evolution; however, this cannot replace the temperature dependency (Whittington et al., 2009).

3. Experimental Results

In this section, we give the depth and lithostatic pressures of buried rocks represented by tracked Lagrangian nodes. Please note that the P-T-t plots include only part of the tracked Lagrangian nodes given in Figure 1 (colored circles) as we select the ones most representative of the numerical model being discussed.

3.1. Numerical Model Evolution and P-T-t Paths for Reference Model

EXP 1 shows the evolution of a numerical experiment in which there is no imposed plate convergence velocity (V_p = 0 cm yr^{-1}) (Figure 2). By 5.5 Myr, the descent of material on the subducting side of the trench (i.e., oceanic lithosphere) tends to drag material from the other side (i.e., continental mantle lithosphere of the upper plate) and an ablative style (double sided) subduction develops (Göğüş, 2015; Tao & O'Connell, 1992). The deformation of the Lagrangian mesh suggests that crustal rocks in the upper plate are also entering into the subduction channel similar to the results of (Gerya & Stöckhert, 2006). The tracked crustal particle in the upper plate (orange, initially at 35 km depth) is buried to 45 km depth with P = 13 kbar and T = 680°C. Crustal particles in the lower plate show small amount of vertical displacement. By 9.7 Myr, the ocean subduction ended and ~200 km of continental material of lower plate has subducted while a portion of ocean lithosphere remains attached to the subducting continent. Crustal material that was initially at 25 km depth in the lower plate (red) is buried to 72 km depth and reaches P = 22 kbar, T = 630°C. The rock that was initially at 15 km depth (green) is buried to 50 km depth and was subjected to P = 15 kbar, T = 480°C. Likewise, the rock that was initially at 10 km depth (blue) is buried to 32 km depth and was subjected to P = 9 kbar, T = 390°C. In contrast, the crustal particle in the upper plate has exhumed, rising to 24 km depth compared to the previous time. This exhumation is partly owing to a decrease in the efficiency of subduction, and partly due to necking of the subducted material which tends to channel the buried rocks to the upper plate. By 14.2 Myr, the ocean slab becomes detached from the continental lithosphere and this results in the removal of vertical forces that were pulling the lithosphere downward. The crustal response to this force-release yields exhumation of buried crustal rocks by 37 km at most (red). The other lower plate rock (green) exhumes 20 km. The rock that shows the least amount of burial (blue) exhumes 7 km. The crust in the overriding plate (orange) continues to exhume (30 km in total), reaching to 13 km below surface.

3.2. Variations in the Plate Convergence Velocity

A series of experiments is conducted to test the influence of plate convergence velocity imposed at the lower plate. The rest of the model parameters are same with EXP 1. In Figure 3, we show model results for (a) EXP 2 (V_p = 1 cm yr^{-1}), (b) EXP 3 (V_p = 2 cm yr^{-1}), and (c) EXP 4 (V_p = 3 cm yr^{-1}) at 14.2 Myr.

In EXP 2, the subduction process develops similarly to the previous experiment (i.e., ablative style). However, the viscous continental mantle lithosphere does not detach from the upper lithosphere. The vertical loading exerted by the descending lithosphere results in deep burial of crustal rock of the lower plate to ~136 km (initially 25 km depth) and reaching the conditions of P = 43 kbar and T = 830°C. Another lower plate crustal particle (green) shows a similar P-T evolution with the previous experiment (i.e., burial to 54 km depth) and

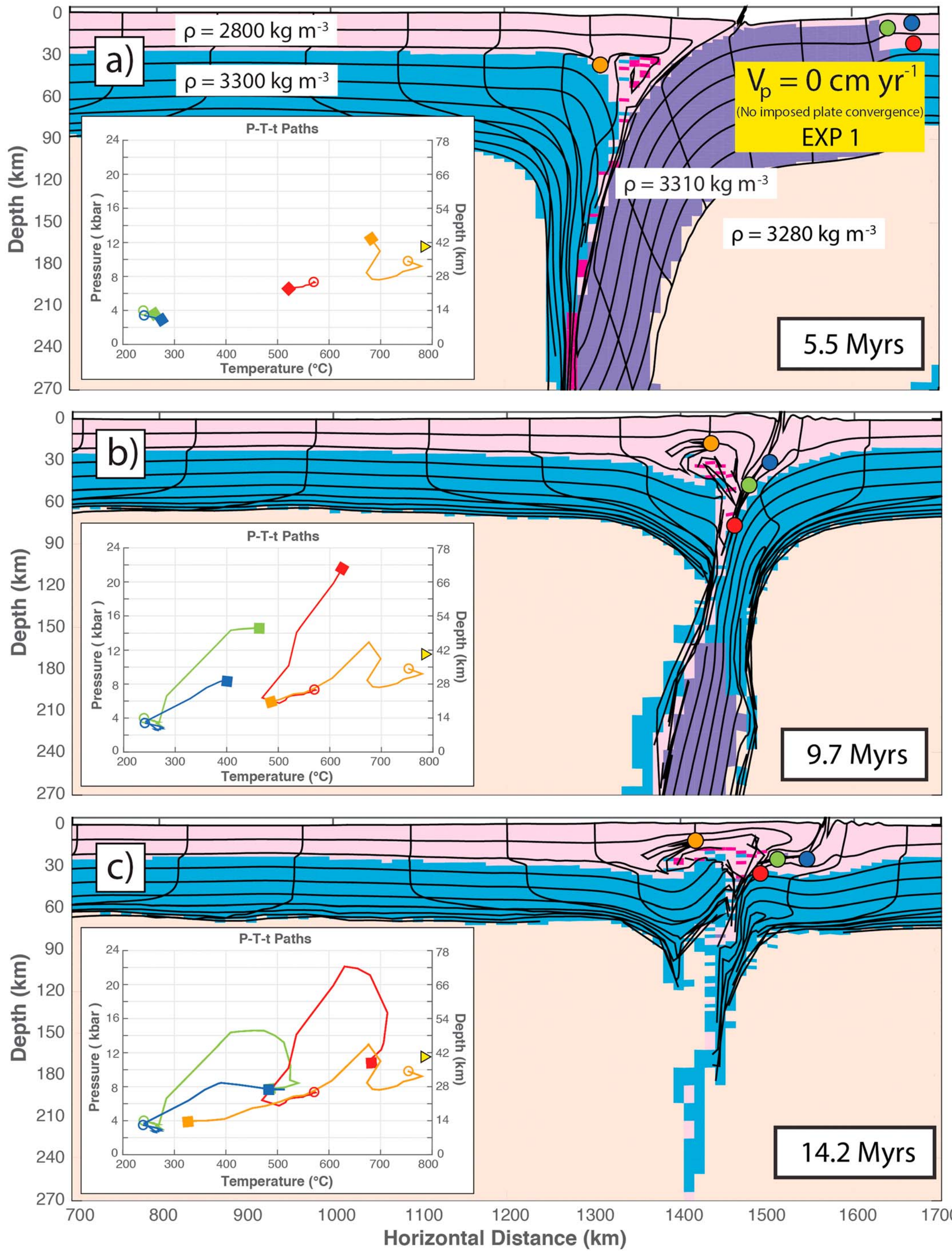

Figure 2. Geodynamic evolution of the reference model (EXP 1) after (a) 5.5 Myrs, (b) 9.7 Myrs, and (c) 14.2 Myrs using viscoplastic (Newtonian creep and no cohesion) continental mantle lithosphere rheology. Pressure-temperature conditions of tracked Lagrangian nodes representative of crustal parcels are shown as insets in each frame. The yellow triangle denotes the approximate 40 km Moho depth, above which the corresponding depth for 1 kbar increment in pressure changes due to density difference between the crust and mantle lithosphere.

P = 16 kbar, T = 490°C. The other lower plate rock (blue) is buried to 39 km depth and have P = 11 kbar, 380°C peak pressure-temperature conditions. However, these particles are not exhumed back to the lower plate, rather they are carried toward the upper plate because of the imposed plate convergence. The particle on the upper plate is buried only 10 km deeper (i.e., from 35 to 45 km depth) with minor variation in the

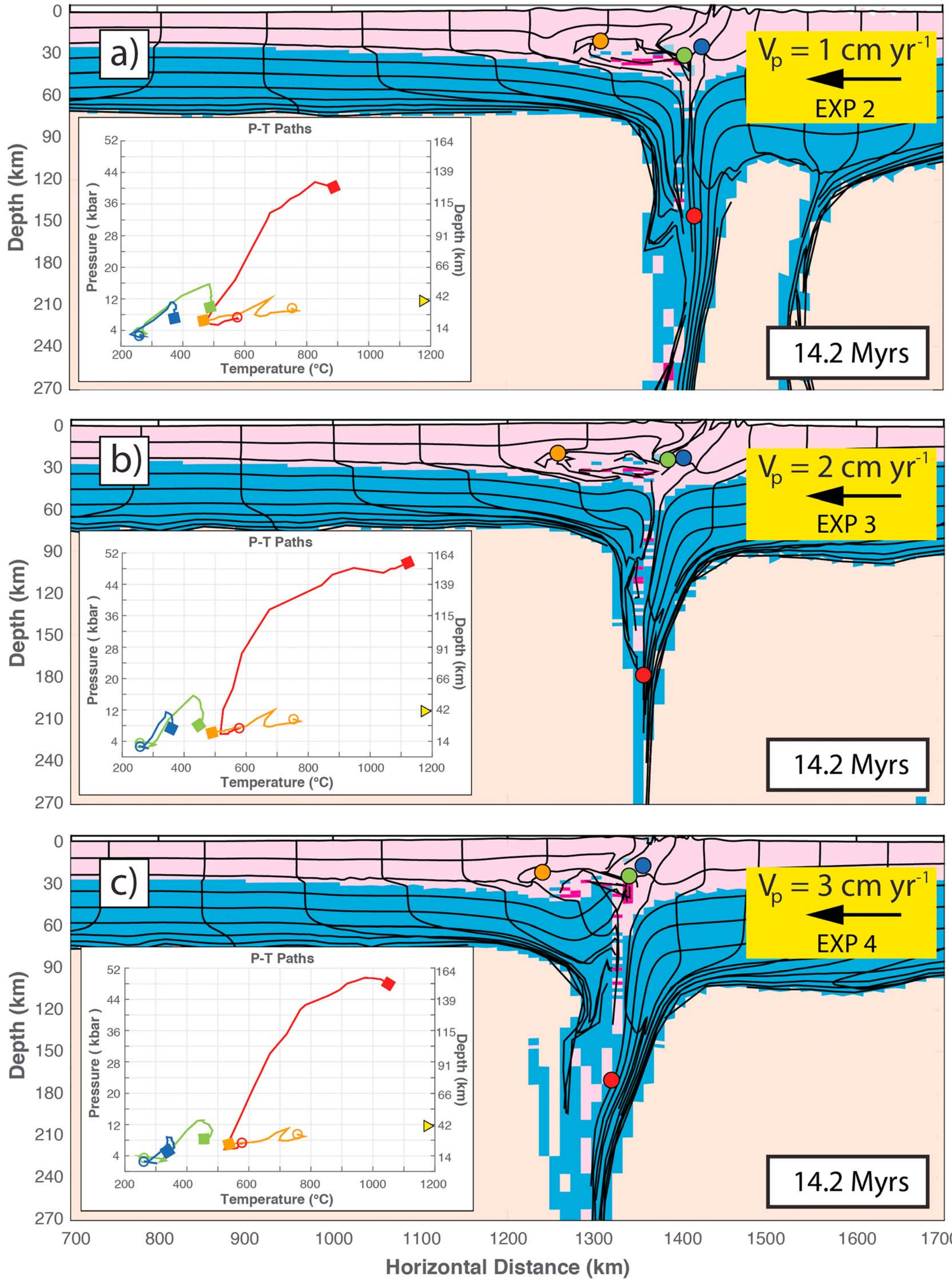

Figure 3. Geodynamic evolution of (a) EXP 2 with plate convergence velocity of 1 cm yr^{-1}, (b) EXP 3 with plate convergence velocity of 2 cm yr^{-1}, and (c) EXP 4 with plate convergence velocity of 3 cm yr^{-1} after 14.2 Myrs using viscoplastic (Newtonian creep and no cohesion) continental mantle lithosphere rheology. The yellow triangle denotes the scale change on the depth-lithostatic pressure relation mentioned on Figure 2 caption.

pressure conditions and small decrease in temperature (i.e., ~300°C in total) since it is not exposed to mantle upwelling under the crust.

Figure 3b shows the P-T variation of EXP 3 where convergence velocity is increased to V_p = 2 cm yr^{-1}. Similarly, the imposed plate convergence promotes deeper subduction of the continental lithosphere

10.1002/2017JB014546

(for both upper and lower plates) and more burial (i.e., to 158 km) of the crust coming from the lower plate (red particle). The higher plate convergence promotes crustal thickening and minor exhumation of the three crustal particles tracked here (orange, green, and blue).

EXP 4 (Figure 3c) shows a similar amount of burial for the deepest subducted continental crust (156 km deep; red) and peak pressure-temperature conditions of P = 50 kbar, T = 970°C. At the same time, the increased convergence causes further shortening and thickening of the crust. The rock that was initially at 15 km depth (green) is buried to 46 km and reaches P = 14 kbar and T = 450°C. Likewise, the rock that was initially at 10 km depth (blue) is buried to 32 km and reaches P = 9 kbar, T = 350°C. The material that was initially at 35 km (orange) is buried to 39 km and have P = 11 kbar, T = 720°C pressure and temperature conditions.

3.3. Variations in Mantle Lithosphere Rheology

In a series of experiments, we explore P-T-t evolution of crustal rocks in subduction to collision models by using only frictional plastic rheology for continental mantle lithosphere of both upper and lower plates (see Table 2 for variation of parameters). Figure 4a shows the evolution of the geodynamic model (EXP 5) with zero plate convergence velocity imposed at the plate boundary.

The results show that oceanic plate subduction is still in progress after 14.2 Myrs of model evolution. The continuity of the subduction is due to the density contrast between the oceanic slab and the underlying asthenospheric mantle. The crustal particle in the upper plate (yellow) is pulled by the subducting oceanic slab down to 50 km depth and is subjected to P = 15 kbar and T = 450°C. The lower plate crustal particles are uplifted to the surface (without any burial) due to foreland bulging in the ocean-continent transition zone. By 25.7 Myrs (Figure 4b), the continental crust of the lower plate has just collided with the crust of the upper plate while necking/thinning of the lower plate occurs at the transition from ocean to continental lithosphere (Figure 4b). Note that the change in the position of the crustal particles is insignificant.

Figure 4c shows EXP 6 with imposed plate convergence velocity of 5 cm yr^{-1}. By 14.2 Myrs, the oceanic plate has already been consumed and continental subduction has progressed. Crustal particles are buried deeper than 25 km in the subduction channel. The crust of upper plate is represented by the deepest subduction (110 km; brown) with P = 35 kbar and T = 750°C. The rocks of the lower plate are buried to 42 km (green), 46 km (red), and 25 km (blue) depths with maximum P-T conditions of 12 kbar, 430°C; 13 kbar, 500°C; and 7 kbar, 320°C, respectively. By 25.7 Myrs, the asthenospheric flow intrudes into the subduction channel. This promotes delamination of the crust from the mantle lithosphere and creates a lithospheric gap (i.e., delamination zone) by ~160 km. The positive buoyancy of the crustal rocks coupled with the asthenospheric flow exhumes the buried rocks to the near surface. In this stage, there is still ongoing convergence supporting crustal thickening at the regions where delamination has not commenced. However, the crust that was exposed to asthenospheric mantle has been appreciably thinned owing to rising mantle flow.

In order to better understand the mechanism for contrasting subduction models, we provide viscosity plots (Figure 5) of EXP 1 at t = 9.7 Myrs and EXP 6 at t = 14.2 Myrs corresponding to highest burial times for each model. In plate-like subduction models where we use only frictional plastic rheology for continental mantle lithosphere, much of the strain is accommodated in the subduction interface during the plate convergence, and the interior of the plate is not exposed to much deformation. This gives an effective isoviscous subducting lithosphere. In this case, the deformation is not purely frictional-plastic and is determined by the upper limit of the viscosity range we defined for the experiments in order to ensure numerical stability. In this setting, the decoupling of the crust and continental mantle lithosphere is minor.

In ablative subduction models where we use a weaker viscoplastic rheology for the continental mantle lithosphere, deformation is more distributed along the interface and strain concentrates along the crust-mantle boundary in both plates. The weakness in rheology facilitates vertical tectonics, and the viscosity structure is clearly distinct from the plate-like subduction case. The contrasting subduction styles result in notable variation in pressure-temperature evolution of the subducted crustal rocks. These models may be similar to the classification of subduction styles as stable versus unstable (Burov & Yamato, 2008), but the P-T predictions are quite different and there are notable differences in the geodynamic evolution.

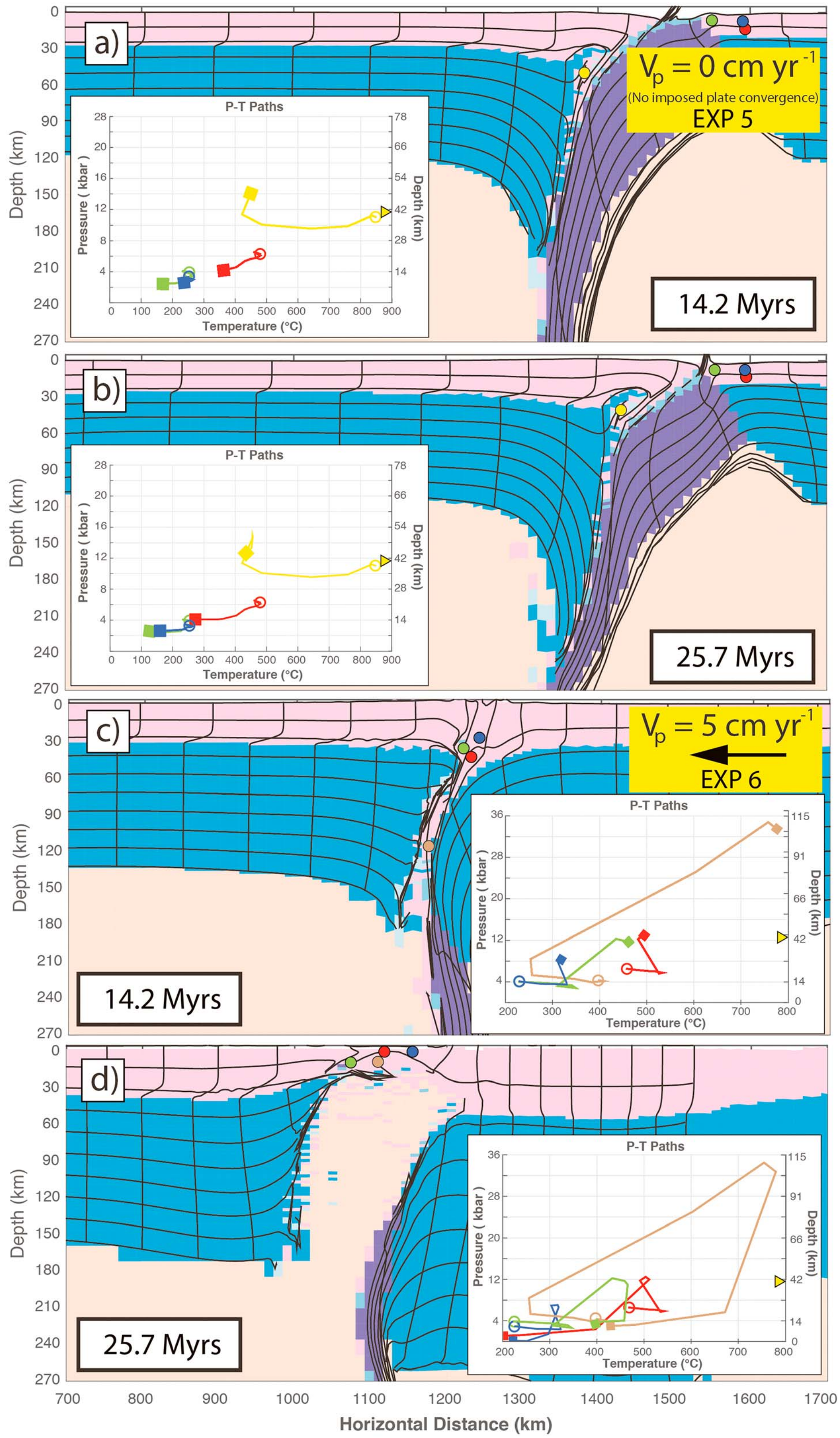

Figure 4. Geodynamic evolution of models using stronger continental mantle lithosphere rheology. (a) EXP 5 after 14.2 Myrs, (b) after 25.7 Myrs with no plate convergence velocity (V_p = 0 cm yr^{-1}), (c) EXP 6 after 14.2 Myrs, and (d) after 25.7 Myrs with a plate convergence velocity of 5 cm yr^{-1}. The yellow triangle denotes the scale change on depth-lithostatic pressure relation mentioned on Figure 2 caption.

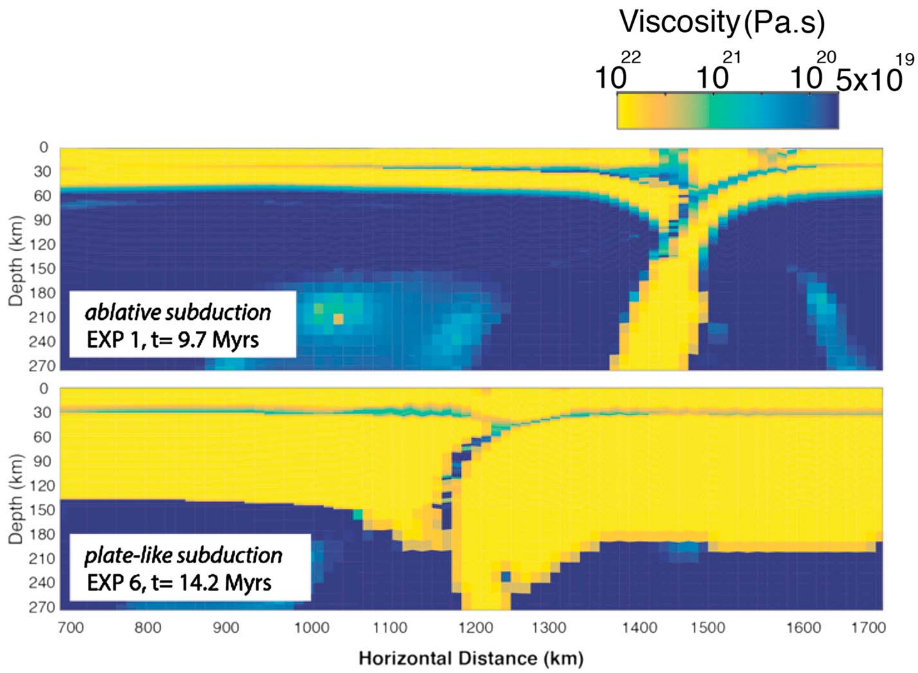

Figure 5. Viscosity plots of EXP 1 at t = 9.7 Myrs and EXP 6 at t = 14.2 Myrs corresponding to the highest burial times for each model.

4. Discussion

The numerical modeling results are compared against thermobarometric P-T estimations from major metamorphic terranes (Figure 6) (see Brown, 2007, for a detailed compilation) and other modeling predictions from a number of sources. The presented models are part of many models (>30) with the same tectonic configuration (i.e., transitioning from oceanic subduction to continental collision). These are selected by assuring that they represent the contrasting tectonic styles among all numerical models (see the supporting information for an overview of all experiments).

Our results show that maximum pressure and temperature conditions in models using viscoplastic rheology for continental mantle lithosphere are generally represented by high-pressure metamorphism and relatively lower temperatures (shown in triangles, P = 9–22 kbar, T = 350°C–630°C) (Figure 6). A similar double-sided subduction was modeled by Sizova et al. (2012) assuming relatively hotter hotter asthenospheric mantle with higher Moho temperature (i.e., >700°C), and weaker felsic continental lower crust. In that work, the tracked crustal rocks are exposed to pressures up to 20 kbar and temperatures around 800°C during the burial process. However, these rocks do not show notable exhumation. Because of the melting process described in their models a lower crustal dome is initiated in the subducting plate and this possibly affects the later stage of the subduction (Sizova et al., 2012). We note that melting is not active in our numerical models.

The modeled pressure and temperature conditions (e.g., purple triangles) of EXP 1 (V_p = 0 cm yr^{-1} so plates can converge freely due to slab-pull force) are in good agreement with P-T estimates from Afyon and Tavşanlı metamorphic zones of western Anatolia. Namely, the modeled P-T variation for the blue particle is P = 9 kbar, 390°C (Figure 2b), and the estimated P-T for the Afyon zone is P = 6–9 kbar, 350°C (Candan et al., 2005). The modeled P-T conditions for the red particle is P = 22 kbar, T = 630°C (Figure 2b), and the P-T estimates for the Tavşanlı zone are P = 24 ± 3 kbar, 430 ± 30°C; (Okay, 2002). We note that such cold exhumation of the Tavşanlı blueschist rocks may well be explained by the dripping of continental lithosphere similar to EXP 1.

Model results with effective isoviscous continental mantle lithosphere and 5 cm yr^{-1} plate convergence velocity (EXP 6) suggest that maximum P-T conditions can reach to the range of ultrahigh-pressure metamorphism (the P-T conditions of brown particle in Figures 4c and 4d is denoted by yellow circle in Figure 6). The modeled P = 35 kbar and T = 750°C conditions are compatible with the P-T approximations for Dora Maira

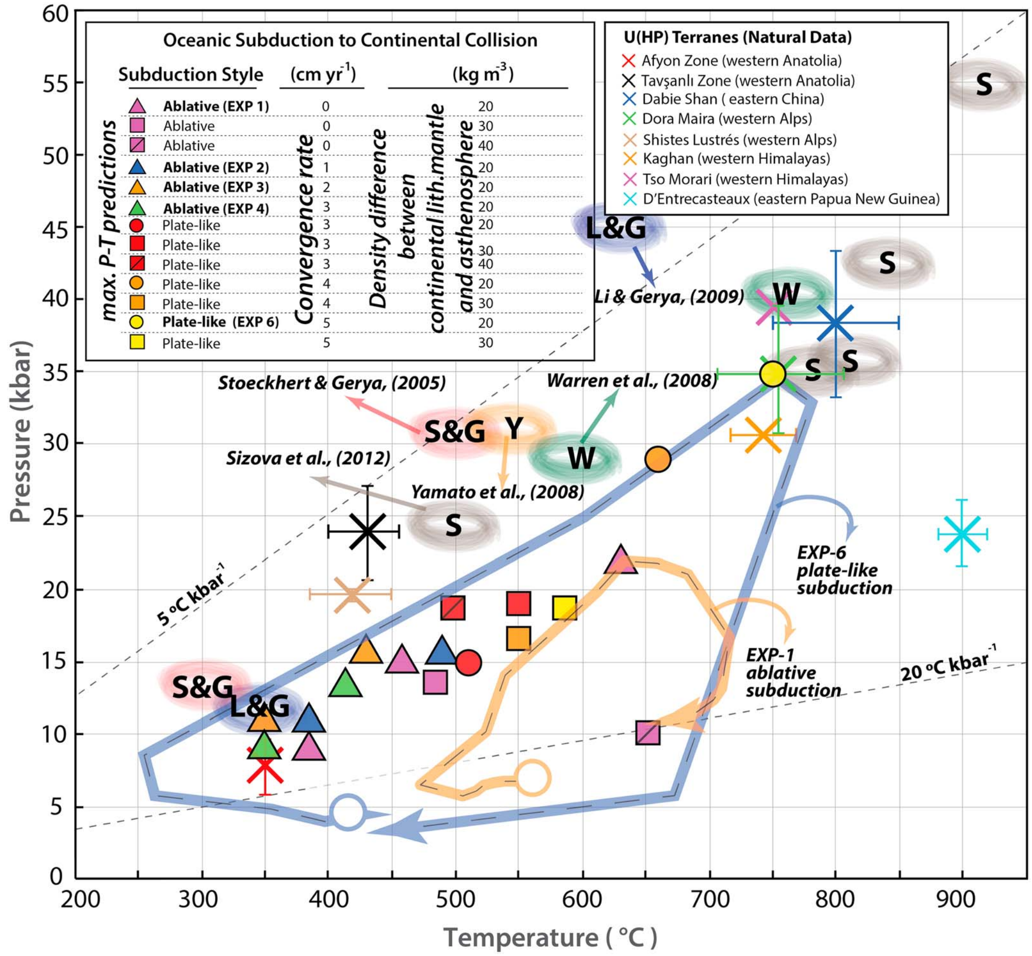

Figure 6. Comparison of peak pressure-temperature conditions of rocks derived from numerical modeling results of this work against thermobarometric data for some of the U(HP) metamorphic belts and other numerical modeling predictions. The circles and triangles represent tracked Lagrangian nodes in the continental crust for the experiments using weak (e.g., hydrated) and strong (e.g., dry) continental mantle lithosphere. We show max. P-T conditions of the most representative rocks in the numerical models. (see Table S1 for other results). The 5°C kbar^{-1} and 20°C kbar^{-1} thermal gradients are given (Brown, 2007). Peak pressure-temperature conditions of rocks are shown as colored crosses with their error bars. Afyon zone: P = 6–9 kbar, T = 350°C (Candan et al., 2005); Tavşanlı zone: P = 24 ± 3 kbar, T = 430 ± 30°C (Okay, 2002), Dabie Shan: P = 38 ± 5 kbar, T = 800 ± 50°C (Okay et al., 1993), Dora Maira: P = 35.5 ± 4 kbar, T = 760 ± 50°C (Rubatto & Hermann, 2001), Kaghan: $P > 27.5$ kbar, T = 720–770°C (Parrish et al., 2006), Shistes Lustrés (i.e., Assietta-Albergian): P = 19–20 kbar, T = 380–450°C (Agard et al., 2001), Tso Morari: $P > 39$ kbar, $T > 750$°C (Mukherjee et al., 2003), and D'Entrecasteaux Islands: P = 20–24 kbar, T = 870°C - 930°C (Baldwin et al., 2004). The references for numerical modeling predictions are L&G (Reference Model): (Li & Gerya, 2009), Y(Figure 7b): (Yamato et al., 2008), W (Model R2-M′-particles h and c, Figure 11a): (Warren, Beaumont, & Jamieson, 2008a), S&G: (Stöckhert & Gerya, 2005). These data are selected to represent the maximum and minimum P_{max}-T conditions predicted in their models.

of western Alps (P = 35.5 ± 4 kbar, T = 760 ± 50°C) (Rubatto & Hermann, 2001), Dabie Shan for eastern China (P = 38 ± 5 kbar, T = 800 ± 50°C) (Okay et al., 1993), and Tso Morari $P > 39$ kbar, $T > 750$°C (Mukherjee et al., 2003), and Kaghan ($P > 27.5$ kbar, T = 720–770°C) (Parrish et al., 2006) in western Himalayas. The predicted exhumation rates in EXP 6 are associated with fast exhumation in the early stage (e.g., 2.8 cm yr^{-1} in 3.21 Myrs) and then an abrupt decrease to 0.47 cm yr^{-1} in the following 3.21 Myrs. This two-stage exhumation process may be consistent with the predicted depth versus time variation in the Dora Maira metamorphic complex, which was measured to be 3.4 cm yr^{-1} in the first 2 Myrs and then 0.87 cm yr^{-1} in the following 3 Myrs (Rubatto & Hermann, 2001). In contrast, this rapid exhumation may not be consistent to preserve the subducted continental rocks in the garnet stability field for greater than 20 Ma, but gives a near-isothermal exhumation similar to the one suggested for the Western Gneiss Region (Kylander-Clark et al., 2012).

The inconsistency of model results with D'Entrecasteaux islands in eastern Papua New Guinea may be explained by significant granodiorite pluton intrusion mainly in an extensional tectonic regime during the exhumation stage of the metamorphic core complex (Hill & Baldwin, 1993). These rocks are exposed to relatively higher temperatures compared to other U(HP) metamorphic rocks (Figure 6). In our numerical models with HP/LT exhumation, the rocks are encased in the continental mantle lithosphere, and asthenospheric intrusion to the crust is not as much as EXP 6. This is consistent with western Anatolia since large granodiorite intrusion has been dated to ~54 Ma which corresponds to the very late stage of the exhumation and may only affect the base of the blueschists (Okay et al., 1998).

The timescale difference between the models (e.g., for EXP 1, burial for ~4 Myrs, exhumation for $>$ 3.5 Myrs) and natural data (e.g., burial for ~10 Myrs and exhumation for $>$ 30 Myrs (Okay et al., 1998)) may be related partly to the limited viscosity range which does not cover below 5×10^{19} Pa s and above 1×10^{22} Pa s in the numerical models. Moreover, at the later stages of exhumation, buried rocks can be uplifted to the surface in much longer period of time and may be driven mainly by surface erosion (Chemenda et al., 1995). That stage is not captured in our models. A more careful analysis should be made by activating the surface erosion.

Our analyses were made by assuming that lithostatic pressures are representative of the burial depths of crustal rocks. However, recent works suggest that notable tectonic overpressures and underpressures (e.g., up to GPa) may be acting on the rocks during the subduction (Gerya, 2015). Therefore, the actual peak pressures may be strikingly different from the lithostatic component. This effect largely depends on the rheology of the lithosphere and may be less efficient in ductile behavior (Gerya, 2015). In our models, we find that the difference in total pressures and lithostatic pressures for the buried crustal rocks vary up to 3.5%, with a better fit in EXP 1. This may be explained by the relative weakness in the rheology of the continental mantle lithosphere.

Furthermore, Yamato & Brun (2017) suggests that the change in tectonic behavior from compression to an extension during plate subduction may lead to a notable decrease in pressures acting on the buried crustal rocks and may not necessarily signify the initiation of the exhumation. Therefore, the classical interpretation of the P-T-t paths may need to be modified accordingly. This may have some effect on our plate-like subduction models as they show the predicted change from compression to an extension. Therefore, the initiation of the exhumation for U(HP) rocks in these models should be taken with more caution. However, the maximum burial depths should be well representative based on the previous arguments.

Although other published works that use numerical modeling to predict P-T-t paths of crustal rocks were able to cover a wide spectrum in P-T space, the absence of UHP exhumation and prevalence of HP/LT exhumation is not well predicted. Some metamorphic terranes have that characteristic (i.e., Afyon and Tavsanli zones in western Turkey), and may be well explained by the ablative subduction case we present in EXP 1. For the UHP exhumation case, our predictions give lower pressures than other modeling studies, but they agree well with natural data from the western Alps, western Himalayas, and eastern China.

It was proposed that shear heating may be the most important secondary process acting on the subducting crust and can be responsible for heating the rocks at shallow depths ($<$20 kbar) (Penniston-Dorland et al., 2015). This idea was based on the difference between mean distribution of P-T prograde paths of U(HP) rocks and numerical modeling predictions. We claim that mantle lithosphere rheology has a primary control on both the subduction style and shear heating process (though not modeled here). We use strain weakening for all layers, and this may strongly lessen the effect of shear heating due to a decrease in the shear stress. A weaker rheology (i.e., EXP 1) would also ensure a lower shear stress in the subduction channel, so it is very hard for these rocks to be heated by such predicted shear. Our models show that P-T paths and maximum P-T values may signify different tectonic evolution for different U(HP) terranes. Therefore, averaging numerous P-T prograde paths of U(HP) rocks belonging to different terranes would remove the intrinsic signal for each region of interest and may result in incorrect interpretations.

5. Conclusions

The model results show that vertical tectonics of transitioning from subduction to a dripping lithosphere can drive efficient burial and exhumation of crustal rocks. Buried crustal rocks can remain encased in ablatively subducting mantle lithosphere and accordingly reach only moderate temperatures. This tectonic style is achieved by using viscoplastic rheology for continental mantle lithosphere. Notably, owing to the effective vertical forcing of the ablatively subducting lithosphere operating at the beginning of oceanic subduction, high-pressure metamorphism occurs without imposed prescribed plate convergence and is mainly driven by vertical tectonics. When we impose plate convergence, models are prone to give a continuous ablative subduction where extreme burial may occur ($>$100 km). The ongoing plate convergence basically promotes only the longevity of the ablative subduction and burial, but does not give much exhumation.

Although the slab break-off/detachment process may seem similar to what we present in our reference model, that refers to a geodynamic process defined by von Blanckenburg and Davies (1995) for the exhumation and magmatism observed in the western Alps. The slab break-off mechanism is associated with detachment of the slab from beneath the subducting (lower) plate itself and presumably do not infer coupling of the lower and upper plates during subduction (Pysklywec et al., 2000). However, both processes (i.e., slab break-off and drips) are controlled by vertical tectonics.

These findings suggest that for the setting of transition from oceanic subduction to continental collision, pressure and temperature conditions of metamorphic rocks may imply the strength of the continental mantle lithosphere. In this regard, ultrahigh-pressure and high-temperature exhumation may correspond to subduction of a coherent slab without causing any disturbance in the upper continental lithospheric mantle (plate-like behavior). This is achieved by using relatively stronger rheology (e.g., dry) for the continental mantle lithosphere. However, high-pressure and low-temperature metamorphic rocks could be indicative of a double-sided (ablative) subduction during which the continental mantle lithosphere from both plates are dragged downward in a weaker viscoplastic rheology (e.g., hydrated), and no ultrahigh-pressure exhumation is observed. In that setting, vertical tectonics may control the burial and exhumation of crustal rocks without necessitating a described far-field plate convergence.

Acknowledgments
Ö.F.B and O.H.G acknowledge funding from The Scientific and Technological Research Council of Turkey (TÜBİTAK) through the project 113Y200. R.N.P. acknowledges funding from an NSERC Discovery Grant. Numerical calculations were done using a modified version of the SOPALE (2000) software. The SOPALE modeling code was originally developed by Philippe Fullsack at Dalhousie University with Chris Beaumont and his Geodynamics group. We acknowledge three anonymous reviewers and Taras Gerya for their constructive comments that greatly improved the manuscript. All model parameters and results are provided in the article and the supporting information. Ö.F.B acknowledges discussions with Gültekin Topuz, Patrice Rey, Greg Houseman, and Geoffrey Clarke.

References

Agard, P., Jolivet, L., & Goffe, B. (2001). Tectonometamorphic evolution of the Schistes Lustres complex: Implications for the exhumation of HP and UHP rocks in western Alps. *Bulletin de la Societe Geologique de France*, *172*, 617–636.

Andersen, T. B., Jamtveit, B., Dewey, J. F., & Swensson, E. (1991). Subduction and eduction of continental crust: Major mechanisms during continent-continent collision and orogenic extensional collapse, a model based on the south Norwegian Caledonides. *Terra Nova*, *3*(3), 303–310. https://doi.org/10.1111/j.1365-3121.1991.tb00148.x

Baldwin, S. L., Monteleone, B. D., Webb, L. E., Fitzgerald, P. G., Grove, M., & Hill, E. J. (2004). Pliocene eclogite exhumation at plate tectonic rates in eastern Papua New Guinea. *Nature*, *431*, 263–267. https://doi.org/10.1038/nature02846

Beaumont, C., Jamieson, R. A., Butler, J. P., & Warren, C. J. (2009). Crustal structure: A key constraint on the mechanism of ultra-high-pressure rock exhumation. *Earth and Planetary Science Letters*, *287*, 116–129. https://doi.org/10.1016/j.epsl.2009.08.001

Beaumont, C., Kamp, P. J. J., Hamilton, J., & Fullsack, P. (1996). The continental collision zone, South Island, New Zealand: Comparison of geodynamical models and observations. *Journal of Geophysical Research*, *101*, 3333–3359. https://doi.org/10.1029/95JB02401

Brown, M. (2007). Metamorphic conditions in orogenic Belts: A record of secular change. *International Geology Review*, *49*, 193–234. https://doi.org/10.2747/0020-6814.49.3.193

Brun, J. P., & Faccenna, C. (2008). Exhumation of high-pressure rocks driven by slab rollback. *Earth and Planetary Science Letters*, *272*, 1–7. https://doi.org/10.1016/j.epsl.2008.02.038

Burov, E., Francois, T., Yamato, P., & Wolf, S. (2014). Mechanisms of continental subduction and exhumation of HP and UHP rocks. *Gondwana Research*, *25*, 464–493. https://doi.org/10.1016/j.gr.2012.09.010

Burov, E., Jolivet, L., Le Lepourhiet, L., & Poliakov, A. (2001). A thermomechanical model of exhumation of HP and UHP metamorphic rocks in Alpine mountain belts. *Tectonophysics*, *342*(1-2), 113–136. https://doi.org/10.1016/S0040-1951(01)00158-5

Burov, E., & Yamato, P. (2008). Continental plate collision, P-T-t-z conditions and unstable vs. stable plate dynamics: Insights from thermo-mechanical modelling. *Lithos*, *103*, 178–204. https://doi.org/10.1016/j.lithos.2007.09.014

Candan, O., Çetinkaplan, M., Oberhänsli, R., Rimmelé, G., & Akal, C. (2005). Alpine high-P/low-T metamorphism of the Afyon Zone and implications for the metamorphic evolution of Western Anatolia, Turkey. *Lithos*, *84*, 102–124. https://doi.org/10.1016/j.lithos.2005.02.005

Chemenda, A. I., Mattauer, M., Malavieille, J., & Bokun, A. N. (1995). A mechanism for syn-collisional rock exhumation and associated normal faulting : Results from physical modelling. *Earth and Planetary Science Letters*, *132*(1-4), 225–232. https://doi.org/10.1016/0012-821X(95)00042-B

Choi, E., Buck, W. R., Lavier, L. L., & Petersen, K. D. (2013). Using core complex geometry to constrain fault strength. *Geophysical Research Letters*, *40*, 3863–3867. https://doi.org/10.1002/grl.50732

Chopin, C. (1984). Coesite and pure pyrope in high-grade blue- schists of the Western Alps: A first record and some consequences. *Contributions to Mineralogy and Petrology*, *86*(2), 107–118. https://doi.org/10.1007/BF00381838

Chopra, P. N., & Paterson, M. S. (1984). The role of water in the deformation of dunite. *Journal of Geophysical Research*, *89*, 7861–7876.

Davies, J. H. (2013). Global map of solid Earth surface heat flow. *Geochemistry, Geophysics, Geosystems*, *14*, 4608–4622. https://doi.org/10.1002/ggge.20271

Duretz, T., & Gerya, T. V. (2013). Slab detachment during continental collision: Influence of crustal rheology and interaction with lithospheric delamination. *Tectonophysics*, *602*, 124–140. https://doi.org/10.1016/j.tecto.2012.12.024

Duretz, T., Gerya, T. V., Kaus, B. J. P., & Andersen, T. B. (2012). Thermomechanical modeling of slab eduction. *Journal of Geophysical Research*, *117*, B08411. https://doi.org/10.1029/2012JB009137

England, P., & Houseman, G. (1989). Extension during continental convergence, with application to the Tibetan Plateau. *Journal of Geophysical Research*, *94*, 17,561–17,579. https://doi.org/10.1029/JB094iB12p17561

Fullsack, P. (1995). An arbitrary Lagrangian-Eulerian formulation for creeping flows and its application in tectonic models. *Geophysical Journal International*, *120*(1), 1–23. https://doi.org/10.1111/j.1365-246X.1995.tb05908.x

Gerya, T. (2015). Tectonic overpressure and underpressure in lithospheric tectonics and metamorphism. *Journal of Metamorphic Geology*, *33*(8), 785–800. https://doi.org/10.1111/jmg.12144

Gerya, T., & Stöckhert, B. (2006). Two-dimensional numerical modeling of tectonic and metamorphic histories at active continental margins. *International Journal of Earth Sciences*, *95*, 250–274. https://doi.org/10.1007/s00531-005-0035-9

Gleason, G. C., & Tullis, J. (1995). A flow law for dislocation creep of quartz aggregates determined with the molten salt cell. *Tectonophysics*, *247*(1-4), 1–23. https://doi.org/10.1016/0040-1951(95)00011-B

Göğüş, O. H. (2015). Rifting and subsidence following lithospheric removal in continental back arcs. *Geology*, *43*(1), 3–6. https://doi.org/10.1130/G36305.1

Göğüş, O. H., & Pysklywec, R. N. (2008a). Mantle lithosphere delamination driving plateau uplift and synconvergent extension in eastern Anatolia. *Geology*, *36*, 723–726. https://doi.org/10.1130/G24982A.1

Göğüş, O. H., & Pysklywec, R. N. (2008b). Near-surface diagnostics of dripping or delaminating lithosphere. *Journal of Geophysical Research*, *113*, B11404. https://doi.org/10.1029/2007JB005123

Göğüş, O. H., Pysklywec, R. N., Corbi, F., & Faccenna, C. (2011). The surface tectonics of mantle lithosphere delamination following ocean lithosphere subduction: Insights from physical-scaled analogue experiments. *Geochemistry, Geophysics, Geosystems*, *12*, Q05004. https://doi.org/10.1029/2010GC003430

Göğüş, O. H., Pysklywec, R. N., & Faccenna, C. (2016). Postcollisional lithospheric evolution of the Southeast Carpathians: Comparison of geodynamical models and observations. *Tectonics*, *35*, 1205–1224. https://doi.org/10.1002/2015TC004096

Göğüş, O. H., Pysklywec, R. N., Şengör, A. M. C., & Gün, E. (2017). Drip tectonics and the enigmatic uplift of the Central Anatolian Plateau. *Nature Communications*, *8*(1), 1538. https://doi.org/10.1038/s41467-017-01611-3

Gray, R., & Pysklywec, R. N. (2012). Geodynamic models of mature continental collision: Evolution of an orogen from lithospheric subduction to continental retreat/delamination. *Journal of Geophysical Research*, *117*, B03408. https://doi.org/10.1029/2011JB008692

Gray, R., & Pysklywec, R. N. (2013). Influence of viscosity pressure dependence on deep lithospheric tectonics during continental collision. *Journal of Geophysical Research: Solid Earth*, *118*, 3264–3273. https://doi.org/10.1002/jgrb.50220

Hacker, B. R., & Gerya, T. V. (2013). Paradigms, new and old, for ultrahigh-pressure tectonism. *Tectonophysics*, *603*, 79–88. https://doi.org/10.1016/j.tecto.2013.05.026

Hill, E. J., & Baldwin, S. L. (1993). Exhumation of high-pressure metamorphic rocks during crustal extension in the D'Entrecasteaux region, Papua New Guinea. *Journal of Metamorphic Geology*, *11*(2), 261–277. https://doi.org/10.1111/j.1525-1314.1993.tb00146.x

Houseman, G. A., & Molnar, P. (1997). Gravitational (Rayleigh-Taylor) instability of a layer with non-linear viscosity and convective thinning of continental lithosphere. *Geophysical Journal International*, *128*(1), 125–150. https://doi.org/10.1111/j.1365-246X.1997.tb04075.x

Kylander-Clark, A. R. C., Hacker, B. R., & Mattinson, C. G. (2012). Size and exhumation rate of ultrahigh-pressure terranes linked to orogenic stage. *Earth and Planetary Science Letters*, *321-322*, 115–120. https://doi.org/10.1016/j.epsl.2011.12.036

Li, Z., & Gerya, T. V. (2009). Polyphase formation and exhumation of high- to ultrahigh-pressure rocks in continental subduction zone: Numerical modeling and application to the Sulu ultrahigh-pressure terrane in eastern China. *Journal of Geophysical Research*, *114*, B09406. https://doi.org/10.1029/2008JB005935

Liao, J., Wang, Q., Gerya, T., & Ballmer, M. D. (2017). Modeling craton destruction by hydration-induced weakening of the upper mantle. *Journal of Geophysical Research: Solid Earth*, *122*, 7449–7466. https://doi.org/10.1002/2017JB014157

Liou, J. G., Tsujimori, T., Zhang, R. Y., Katayama, I., & Maruyama, S. (2004). Global UHP metamorphism and continental subduction/collision: The Himalayan model. *International Geology Review*, *46*, 1–27. https://doi.org/10.2747/0020-6814.46.1.1

Liu, X., Wei, C., Li, S., Dong, S., & Liu, J. (2004). Thermobaric structure of a traverse across western Dabieshan: Implications for collision tectonics between the Sino-Korean and Yangtze cratons. *Journal of Metamorphic Geology*, *22*(4), 361–379.

Massonne, H. J. (2003). A comparison of the evolution of diamondiferous quartz-rich rocks from the Saxonian Erzgebirge and the Kokchetav Massif: Are so-called diamondiferous gneisses magmatic rocks? *Earth and Planetary Science Letters*, *216*(3), 347–364. https://doi.org/10.1016/S0012-821X(03)00512-0

Molnar, P., Houseman, G. A., & Conrad, C. P. (1998). Rayleigh-Taylor instability and convective thinning of mechanically thickened lithosphere: Effects of non-linear viscosity decreasing exponentially with depth and of horizontal shortening of the layer. *Geophysical Journal International*, *133*(3), 568–584. https://doi.org/10.1046/j.1365-246X.1998.00510.x

Mukherjee, B. K., Sachan, H. K., Ogasawara, Y., Muko, A., & Yoshioka, N. (2003). Carbonate-bearing UHPM rocks from the Tso-Morari region, Ladakh, India: Petrological implications. *International Geology Review*, *45*(1), 49–69. https://doi.org/10.2747/0020-6814.45.1.49

Okay, A., & Şengör, A. M. C. (1992). Evidence for intracontinental thrust-related exhumation of the ultra-high-pressure rocks in China. *Geology*, *20*(5), 411–414. https://doi.org/10.1130/0091-7613(1992)020%3C0411

Okay, A. I. (2002). Jadeite–chloritoid–glaucophane–lawsonite blueschists in north-west Turkey: Unusually high P/T ratios in continental crust. *Journal of Metamorphic Geology*, *20*(8), 757–768. https://doi.org/10.1046/j.1525-1314.2002.00402.x

Okay, A. I., Harris, N. B. W., & Kelley, S. P. (1998). Exhumation of blueschists along a Tethyan suture in northwest Turkey. *Tectonophysics*, *285*(3-4), 275–299. https://doi.org/10.1016/S0040-1951(97)00275-8

Okay, A. I., Şengör, A. M. C., & Satır, M. (1993). Tectonics of an ultrahigh-pressure metamorphic terrane: The Dabie Shan/Tongbai Shan orogen, China. *Tectonics*, *12*(6), 1320–1334. https://doi.org/10.1029/93TC01544

O'Reilly, S. Y., Griffin, W. L., Djomani, Y. H. P., & Morgan, P. (2001). Are lithospheres forever? *GSA Today*, *11*(4), 4–10. https://doi.org/10.1130/1052-5173(2001)011%3C0004:ALFTCI%3E2.0.CO;2

Parrish, R. R., Gough, S. J., Searle, M. P., & Waters, D. J. (2006). Plate velocity exhumation of ultrahigh-pressure eclogites in the Pakistan Himalaya. *Geology*, *34*(11), 989–992. https://doi.org/10.1130/G22796A.1

Penniston-Dorland, S. C., Kohn, M. J., & Manning, C. E. (2015). The global range of subduction zone thermal structures from exhumed blueschists and eclogites: Rocks are hotter than models. *Science Letters*, *428*, 243–254. https://doi.org/10.1016/j.epsl.2015.07.031

Plunder, A., Agard, P., Chopin, C., Pourteau, A., & Okay, A. I. (2015). Accretion, underplating and exhumation along a subduction interface: From subduction initiation to continental subduction (Tavşanlı zone, W. Turkey). *Lithos*, *226*, 233–254. https://doi.org/10.1016/j.lithos.2015.01.007

Pourteau, A., Sudo, M., Candan, O., Lanari, P., Vidal, O., & Oberhänsli, R. (2013). Neotethys closure history of Anatolia: Insights from ^{40}Ar-^{39}Ar geochronology and P-T estimation in high-pressure metasedimentary rocks. *Journal of Metamorphic Geology*, *31*(6), 585–606. https://doi.org/10.1111/jmg.12034

Pysklywec, R. N., Beaumont, C., & Fullsack, P. (2000). Modeling the behavior of the continental mantle lithosphere during plate convergence. *Geology*, *28*(7), 655–658. https://doi.org/10.1130/0091-7613(2000)28%3C655:MTBOTC%3E2.0.CO
Pysklywec, R. N., Beaumont, C., & Fullsack, P. (2002). Lithospheric deformation during the early stages of continental collision: Numerical experiments and comparison with South Island, New Zealand. *Journal of Geophysical Research*, *107*(B7), 2133. https://doi.org/10.1029/2001JB000252
Pysklywec, R. N., & Cruden, A. R. (2004). Coupled crust-mantle dynamics and intraplate tectonics: Two-dimensional numerical and three-dimensional analogue modeling. *Geochemistry, Geophysics, Geosystems*, *5*, Q10003. https://doi.org/10.1029/2004GC000748
Pysklywec, R. N., Gogus, O., Percival, J., Cruden, A. R., & Beaumont, C. (2010). Insights from geodynamical modeling on possible fates of continental mantle lithosphere: Collision, removal, and overturn. *Canadian Journal of Earth Sciences*, *47*, 541–563. https://doi.org/10.1139/E09-043
Rubatto, D., & Hermann, J. (2001). Exhumation as fast as subduction? *Geology*, *29*(1), 3–6. https://doi.org/10.1130/0091-7613(2001)?029%3C0003:EAFAS%3E?2.0.CO
Sherlock, S., Kelley, S., Inger, S., Harris, N., & Okay, A. (1999). 40Ar-39Ar and Rb-Sr geochronology of high-pressure metamorphism and exhumation history of the Tavsanli zone, NW Turkey. *Contributions to Mineralogy and Petrology*, *149*(6), 699–712. https://doi.org/10.1007/s00410-005-0676-5
Sizova, E., Gerya, T., & Brown, M. (2012). Exhumation mechanisms of melt-bearing ultrahigh pressure crustal rocks during collision of spontaneously moving plates. *Journal of Metamorphic Geology*, *30*, 927–955. https://doi.org/10.1111/j.1525-1314.2012.01004.x
Sobolev, N. V., & Shatsky, V. S. (1990). Diamond inclusions in garnets from metamorphic rocks: A new environment for diamond formation. *Nature*, *343*, 742.
Stöckhert, B., & Gerya, T. V. (2005). Pre-collisional high pressure metamorphism and nappe tectonics at active continental margins: A numerical simulation. *Terra Nova*, *17*, 102–110. https://doi.org/10.1111/j.1365-3121.2004.00589.x
Tao, W. C., & O'Connell, R. J. (1992). Ablative Subduction : A two-sided subduction alternative model to the conventional. *Journal of Geophysical Research*, *97*(B6), 8877–8904. https://doi.org/10.1029/91JB02422
Terry, M. P., & Robinson, P. (2004). Geometry of eclogite-facies structural features: Implications for production and exhumation of ultrahigh-pressure and high-pressure rocks, Western Gneiss Region, Norway. *Tectonics*, *23*, TC2001. https://doi.org/10.1029/2002TC001401
Tirel, C., Brun, J. P., Burov, E., Wortel, M. J. R., & Lebedev, S. (2013). A plate tectonics oddity: Caterpillar-walk exhumation of subducted continental crust. *Geology*, *41*(5), 555–558. https://doi.org/10.1130/G33862.1
von Blanckenburg, F., & Davies, J. H. (1995). Slab breakoff: A model for syncollisional magmatism and tectonics in the Alps. *Tectonics*, *14*, 120–131. https://doi.org/10.1029/94TC02051
Warren, C. J. (2013). Exhumation of (ultra-)high-pressure terranes: Concepts and mechanisms. *Solid Earth*, *4*(1), 75–92. https://doi.org/10.5194/se-4-75-2013
Warren, C. J., Beaumont, C., & Jamieson, R. A. (2008a). Deep subduction and rapid exhumation : Role of crustal strength and strain weakening in continental subduction and ultrahigh-pressure rock exhumation. *Tectonics*, *27*, TC6002. https://doi.org/10.1029/2008TC002292
Warren, C. J., Beaumont, C., & Jamieson, R. A. (2008b). Modelling tectonic styles and ultra-high pressure (UHP) rock exhumation during the transition from oceanic subduction to continental collision. *Earth and Planetary Science Letters*, *267*, 129–145. https://doi.org/10.1016/j.epsl.2007.11.025
Whittington, A. G., Hofmeister, A. M., & Nabelek, P. I. (2009). Temperature-dependent thermal diffusivity of the Earth's crust and implications for magmatism. *Nature*, *458*, 319–321. https://doi.org/10.1038/nature07818
Willett, S., Beaumont, C., & Fullsack, P. (1993). A mechanical model for the tectonics of doubly-vergent compressional orogens. *Geology*, *21*(4), 371–374. https://doi.org/10.1130/0091-7613(1993)021%3C0371:MMFTTO%3E2.3.CO
Yamato, P., Agard, P., Burov, E., Le Pourhiet, L., Jolivet, L., & Tiberi, C. (2007). Burial and exhumation in a subduction wedge: Mutual constraints from thermomechanical modeling and natural P-T-t data (Schistes Lustres, western Alps). *Journal of Geophysical Research*, *112*, B07410. https://doi.org/10.1029/2006JB004441
Yamato, P., & Brun, J. P. (2017). Metamorphic record of catastrophic pressure drops in subduction zones. *Nature Geoscience*, *10*(1), 46–50. https://doi.org/10.1038/ngeo2852
Yamato, P., Burov, E., Agard, P., Le Pourhiet, L., & Jolivet, L. (2008). HP-UHP exhumation during slow continental subduction: Self-consistent thermodynamically and thermomechanically coupled model with application to the Western Alps. *Earth and Planetary Science Letters*, *271*, 63–74. https://doi.org/10.1016/j.epsl.2008.03.049